

A simple and convenient preparation of flexible paper-Ag NPs substrate for surface enhanced Raman spectroscopy

Yilan Lu^{1,a,*}

¹Key Laboratory of Optoelectronic Chemical Materials and Devices, Ministry of Education,
College of Optoelectronic Materials and Technology, Jiangnan University, Wuhan, China

^a3179972020@qq.com

*Corresponding author

Keywords: Surface enhanced Raman spectroscopy (SERS); In-situ synthesis; Paper-Ag NPs; R6G; Ciprofloxacin (CIP)

Abstract: In recent years, flexible SERS substrates based on cellulosic materials have been widely investigated. In this study, paper was dissolved and dispersed in an alkaline solution, and Ag NPs were synthesised in situ on cleaned paper scraps, which were dried to form a complete paper SERS substrate. The whole preparation process is simple, the preparation time is short, and the Ag NPs are uniformly distributed inside and outside the paper, which can be arbitrarily cut and extracted by wiping the analyte surface, which is convenient for liquid sample detection. Most importantly, the substrate overcomes the problem of paper dissolution and damage due to immersion. The detection of 10^{-7} M R6G was achieved with enhancement factor of 1.95×10^5 . The Raman activity was still present after 60 days of refrigerated storage. The reproducibility was good (RSD = 9.5 %). And now the substrate has been successfully used for the detection of ciprofloxacin in water, with the detection limits of 2.2×10^{-4} M.

1. Introduction

Surface enhanced Raman spectroscopy (SERS), a vibrational spectroscopic technique, can be used to identify a wide range of molecules on a trace level in a stable, fast and non-destructive manner[1,2]. Therefore, it has been widely applied in the fields of food safety[3,4], environment[5,6], pharmaceuticals[7,8] and medicine[9,10]. However, it is difficult to find a suitable SERS substrate because of the low reproducibility and the high variation of the SERS signal, which is affected by the conformation of the metal nanoparticles. To overcome these drawbacks of SERS, various methods have been developed to prepare suitable nanostructures, such as the construction of SERS substrates by electrochemical deposition[11], vapour deposition[12], e-beam lithography[13] and colloidal lithography[14] on conventional solid supports such as glass[15], silicon[16], zinc oxide (ZnO)[17,18], polymers[19,20], carbon nanotubes (CNTs)[21], anodic aluminium oxide (AAO)[22] and polydimethylsiloxane (PDMS)[23,24]. The substrates produced by these methods are rigid and have a high degree of reproducibility and sensitivity. However, the fabrication process of these substrates is extremely complicated, the cost

of mass production is too high, environmental pollution may be caused during the fabrication process, and the rigid substrates are not suitable for direct SERS detection of samples with irregular morphology, so the substrates have their own practical limitations. Therefore, there is a need for the development of SERS substrates which are low cost, simple and easy to fabricate[25-27].

In recent years, flexible SERS substrates on the basis of cellulose materials have been widely investigated, and paper has been the material of choice for the majority of substrate preparation studies. Paper, with its flexible morphology and geometry that can be adapted to specific needs, is an inexpensive, portable and widely available material. It offers the advantages of being inexpensive, eco-friendly, biodegradable and commercially available[26]. Furthermore, paper based SERS substrates are more conducive to forming “hot spots” due to the porous structure of the paper surface, which enhances the intensity of Raman signals. Currently, drip-coating, impregnation, in-situ synthesis, in-kjet printing, spraying and writing are the main methods used to fabricate paper based SERS substrates. However, using paper as a substrate is also limited by the following: Impregnation takes a long time to prepare and can cause paper to swell and deteriorate[28]; nanoparticles tend to oxidise during inkjet printing, and printing costs can be prohibitive (Table 1). Thus, simple, homogeneous and stable paper SERS substrates need to be developed.

Table 1: Preparation of paper-based SERS substrates.

| Methods of synthesis | The advantages | The disadvantages | Citations |
|----------------------|--|--|-----------|
| Drip coating | Easy to operate. | Uniformity is difficult to control | [25,29] |
| Impregnation | | Long preparation time, cellulose paper base is easily swollen | [9,30] |
| In-situ synthesis | Controlled uniformity. | -- | [31,32] |
| Ink-jet printing | Ag NPs can be evenly distributed on the paper and the signal is very stable. | Nanoparticles tend to oxidise, requiring the nanoparticle solution in the cartridge to be replaced, and the replacement process is cumbersome, nanoparticles can easily clog the printer's printhead, causing damage to the machine, The costs are high. | [26,33] |
| Spraying | Low cost, simple operation and short preparation time. | Several coats are required to achieve the desired effect and the paper must be surface modified. | [34,35] |

Ciprofloxacin (CIP) is a fluoroquinolone antibiotic of the third generation[36]. It is highly potent and has a broad spectrum of antibacterial activity, which makes it widely used in both human and veterinary medicine. Currently, the misuse of antibiotics is significant and can be a major source of contamination of soil and natural waters[37]. High levels of antibiotics in ecological systems can lead to the development of antibiotic resistance, and it is important to monitor CIP levels in ecological systems as it is one of the most efficient antibiotics in the treatment of bacterial infections[38]. CIP can be quantified by high-performance liquid chromatography (HPLC) and thin-layer chromatography (TLC), according to pharmacopoeias and the pharmaceutical industry[39]. However, both methods are time-consuming and destructive to the sample, and the reagents are expensive and time-consuming. Therefore, there is a need for analytical methods such as SERS. These methods are fast and do not require complex sample pretreatment [39,40].

In the present study, the paper was dissolved and distributed in alkaline solution, and Ag NPs synthesized in situ on the cleaned paper shreds, dried to form a complete paper SERS substrate. The whole preparation process is simple, the preparation time is short, and the Ag NPs are uniformly distributed inside and outside the paper, which can be cut as desired and extracted by wiping the surface with the analyte, facilitating the detection of liquid samples. In particular, it overcomes the problem of paper swell and damage caused by immersion. The substrate has now been successfully used to detect ciprofloxacin in water.

2. Manuscript Preparation

2.1. Chemicals and Equipment

All chemicals were in analytical grade. Urea ($\text{CH}_4\text{N}_2\text{O}$, 99 %), Sodium hydroxide (NaOH , 96 %), Acetic acid ($\text{C}_2\text{H}_4\text{O}_2$, 99 %), silver nitrate (AgNO_3 , 99.8 %), hydroxylamine hydrochloride ($\text{NH}_2\text{OH HCl}$, 99.0 %) were purchased from Sinopharm Chemical Reagent Co. (Shanghai, China); Rhodamine 6G (R6G, 99.9 %) was obtained from Aladdin; and ciprofloxacin (CIP) was purchased from Zhejiang countries the state pharmaceutical co. (zhejiang, China); Ultrapure water was purified by ELGA Flex 2.

The scanning electron microscope (SEM) images were recorded on a SU8010 Hitachi instrument. All SERS spectra were acquired directly by Renishaw in Via-Reflex.

2.2. Preparation of paper-Ag NPs SERS substrate

The paper-AgNPs SERS substrate is the result of a combination of N. Leopold [41] and Lina Zhang [42]. In detail, The Mixed solution of $\text{NaOH}/\text{CH}_4\text{N}_2\text{O}/\text{H}_2\text{O}$ (7: 12: 81 by mass) was first prepared and cooled to $-20\text{ }^\circ\text{C}$. Tissue paper was added to this mixture and stirred vigorously for 30 min. Place 8 g of paper glue in a 50 mL centrifuge tube, add 30 mL of dilute acetic acid, shake and rinse several times with ultrapure water. Then, add 30 mL AgNO_3 ($1.11 \times 10^{-3}\text{ M}$), shake for 30 minutes, centrifuge for 5 minutes, discard the supernatant, add AgNO_3 ($1.11 \times 10^{-3}\text{ M}$) and hydroxylamine hydrochloride/sodium hydroxide ($1.5 \times 10^{-2}\text{ M}/3 \times 10^{-2}\text{ M}$) in sequence, shake for 30 minutes, centrifuge for 5 minutes, discard the supernatant and transfer the paper base to a 60 mm Petri dish. After thawing at room temperature, the supernatant was discarded and dried at $60\text{ }^\circ\text{C}$.

2.3. SERS detection

Preparation of different concentrations ($1 \times 10^{-5}\text{ M}$ -- $1 \times 10^{-8}\text{ M}$) of R6G solution, basal area of $0.5 \times 0.5\text{ cm}^2$, addition of 100 μL R6G, SERS signals were collected after 20 min. Laser wavelength 785 nm, laser power 5 mW, integration time 10 s, cumulative frequency 1 times, magnification 50×20 .

By dissolving 0.5 g of the sample powder in hydrochloric acid solution (0.12 M, 25 mL) and diluting, different concentrations of CIP solutions (4.75×10^{-2} -- $4.75 \times 10^{-5}\text{ M}$, $2.2 \times 10^{-4}\text{ M}$) were prepared. The SERS detection like R6G.

3. Results and discussion

3.1. Optimization and Characterization of the paper-Ag NPs

As can be seen in figure 1a, the prepared substrate does not have any obvious Raman peaks in the range of $500\text{--}2000\text{ cm}^{-1}$, so that Raman peaks in this range can be detected and identified with a low level of background interference. The in-situ synthesis of Ag NPs was performed on a smaller area of the paper, such that the entire paper substrate had Ag NPs (both inside and outside) (Fig. 1c,d). And the whole preparation process was simple, took a short time and solved the problem of paper dissolution damage caused by immersion.

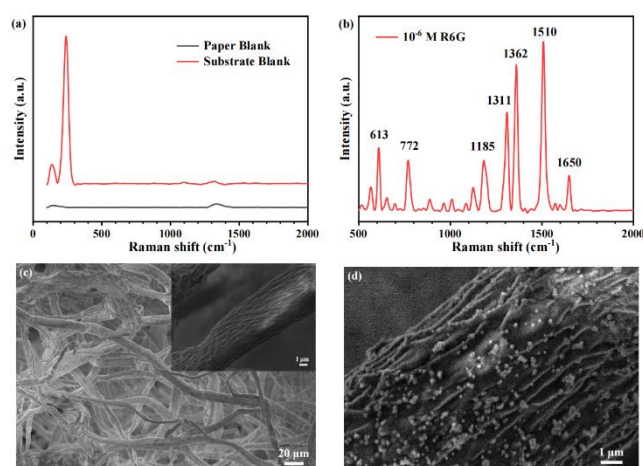


Figure 1: The Raman spectra and SEM of paper substrate with and without Ag NPs (a,c,d). (b) The Raman spectra of R6G (10^{-6} M) on the paper-AgNPs.

After initial optimisation, the substrate was optimised by varying these two conditions, as it was found that the pH of the reducing agent and the number of layers of Ag NPs had a significant effect on reducing the detection limit and increasing the enhancement factor. However, the volume of the centrifuge tube was different from the volume measured with the measuring cylinder and varied significantly. However, both can achieve similar enhancement effects. The only differences are in the operating procedures.

The figure 1b shows the Raman spectra of R6G on the fabricated substrates. Typical Raman peaks for rhodamine 6G are seen at 613, 772, 1185, 1311, 1362, 1510 and 1650 cm^{-1} . Each peak can be assigned as follows: 613 cm^{-1} for the in-plane bending mode of the C–C ring, 772 and 1185 cm^{-1} for the out-of-plane bending and in-plane bending modes of the C–H ring, and 1311, 1360, 1510 and 1650 cm^{-1} for the tensile modes of the aromatic ring (Table 2)[2,43,44]. The peaks of R6G at 1510 cm^{-1} were selected to assess the performance of the substrate. The enhancement was quantified using equation (1).

$$AEF = \frac{I_{SERS} C_{Normal}}{I_{Normal} C_{SERS}} \quad (1)$$

where I_{SERS} is the SERS intensity of R6G on the plasmonic paper, C_{SERS} is the concentration of R6G on the plasmonic paper, I_{Raman} is the Raman intensity of R6G on the paper without Ag NPs, and C_{Raman} is the concentration of R6G on the paper without Ag NPs.

Table 2: Main Raman characteristic peaks and band assignments of R6G[2,43,44]

| SERS (cm^{-1}) | Band assignment |
|---------------------------|--|
| 613 | in-plane bending mode of the C–C ring |
| 772 | out-of-plane bending modes of the C–H ring |
| 1185 | in-plane bending modes of the C–H ring |
| 1311 | tensile modes of the aromatic ring |
| 1362 | tensile modes of the aromatic ring |
| 1510 | tensile modes of the aromatic ring |
| 1650 | tensile modes of the aromatic ring |

3.1.1. Preparation of paper-Ag NPs in centrifuge tubes

The Ag NPs were synthesised in situ on waste paper using hydroxylamine hydrochloride/sodium

hydroxide solution (1.5×10^{-2} M/ 3×10^{-2} M) at pH = 7 and AgNO₃ (1.11×10^{-3} M). The reaction was performed in centrifuge tubes and then dried to obtain paper-Ag NPs. The SERS performance was measured with R6G. The detection limit of 10^{-5} M R6G was obtained and the enhancement factor of 2.63×10^3 for the SERS substrate at 1510 cm^{-1} (Fig. 2a). Increasing the number of Ag NPs, which is increasing the number of reactions, finally reduced the detection limit to 10^{-6} M, reaching the enhancement factor of 1.75×10^5 with four layers of particles (Fig. 2b,c). pH is another factor affecting the SERS enhancement, and the figure 2d shows that with increasing pH, the enhancement was greatest at pH = 10 and one layer of particles, with the enhancement factor of 3.57×10^4 and the detection limit of 10^{-7} M (Fig. 3). Figure 4 shows The SEM of paper-Ag NPs with different number of Ag NPs with pH = 7, the layer of 1-5 and pH = 10, 1 layer. In the fifth layer, the increasing number of Ag NP causes the particles to aggregate and the Raman intensity to weaken.

3.1.2. Preparation of paper-Ag NPs with 9: 1

When the volume ratio of AgNO₃ solution and hydroxylamine hydrochloride/sodium hydroxide solution was 9: 1, the enhancement diminished with increasing pH (Fig. 5a). The graph shows that the enhancement was greatest at pH = 7 and a quantity of 120 mL of Ag NPs, with the enhancement factor of 1.95×10^5 and the detection limit of 10^{-6} M (Fig. 5). Furthermore, as the number of Ag NPs increases, aggregation of the nanoparticles occurs during stirring, resulting in a weakening of the SERS enhancement at 160 mL and 200 mL particle number (Fig. 6d, e).

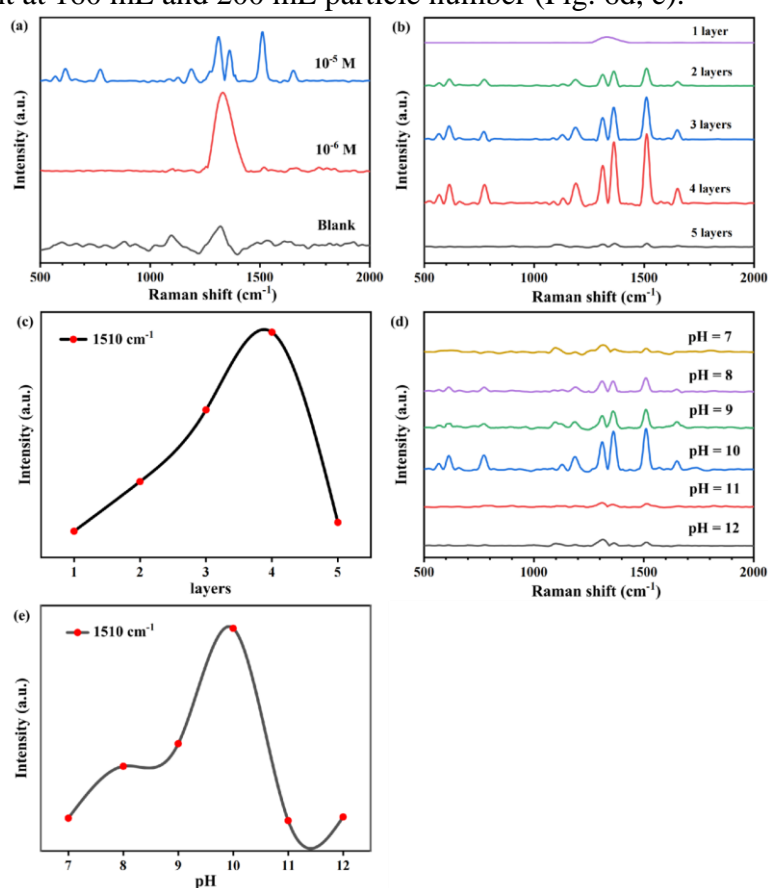
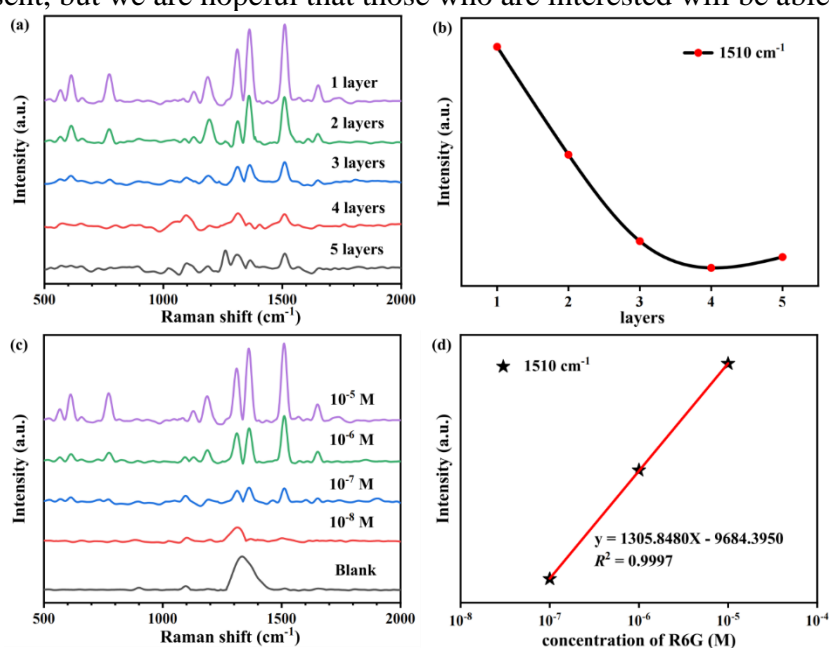


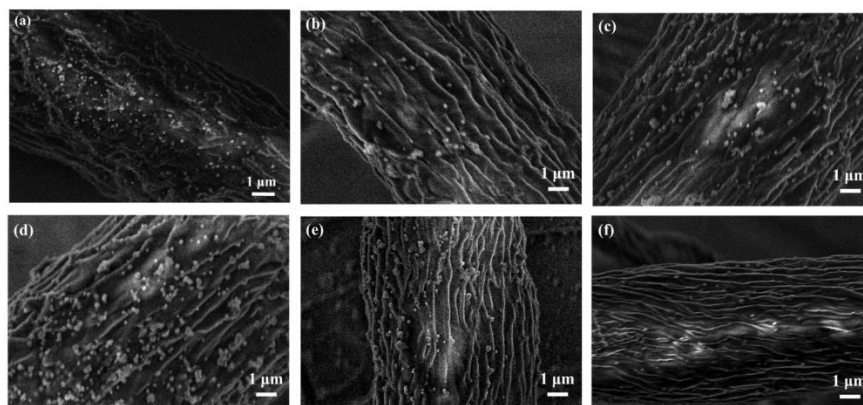
Figure 2: The SERS spectra of paper-Ag NPs were prepared in centrifuge tubes with R6G, hydroxylamine hydrochloride/sodium hydroxide solution pH = 7. (a) 1 layer of Ag NPs. (b, c) Relationship of Raman signal with increasing number of nanoparticle layers (1--5). (d) Relationship of Raman signal with pH (7--12).

As we all know, the size, shape, curvature and number of the nanoparticles, the size or morphology of the gaps between the nanoparticles and the angle of formation can be altered by changing the reaction conditions, which will affect the SERS intensity[45]. During the optimisation process, we changed the amount of reductant and oxidant added, the pH of the reductant and the concentration of the oxidant AgNO_3 by controlling the variables. Finally, we found some of the above results. However, the detection limit of the substrate for R6G is as low as 10^{-7} M. From the Figure 7, we can see that increasing the concentration of AgNO_3 to 10^{-2} M reduces the detection limit of R6G to 10^{-9} M, but the characteristic peaks are all shifted left by about 100 cm^{-1} (Fig. 7). Due to our lack of knowledge of Raman spectroscopy, we do not have an explanation for this phenomenon at present, but we are hopeful that those who are interested will be able to explain it.



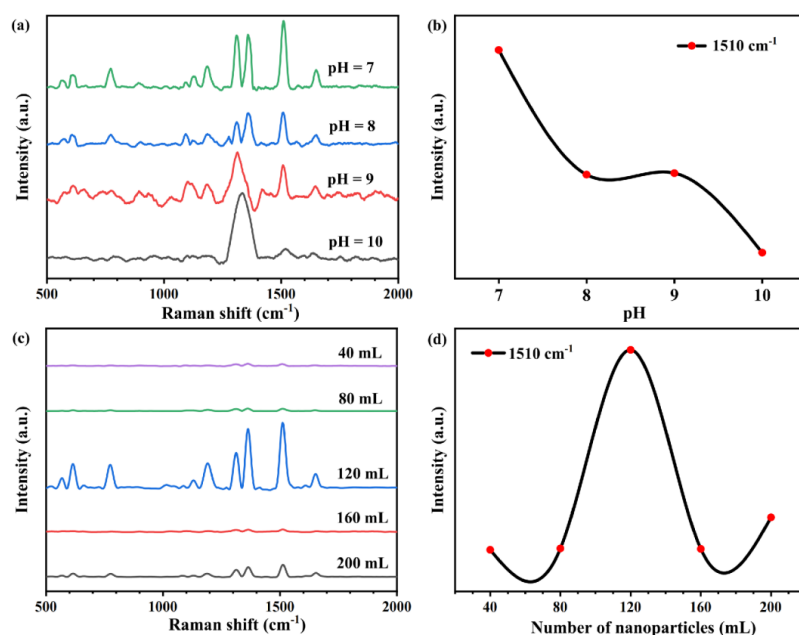
(a, b) Relationship of Raman signal with increasing number of nanoparticle layers (1-5). (c) Concentration-dependent SERS detection of R6G from 10^{-5} to 10^{-7} M. (d) The linear correlation of Raman intensity at 1510 cm^{-1} with the concentration changing from 10^{-5} to 10^{-7} M.

Figure 3: The SERS spectra of paper-Ag NPs were prepared in centrifuge tubes with R6G, hydroxylamine hydrochloride/sodium hydroxide solution pH = 10.



(a,b,c,d,e) pH = 7, the layer of 1--5. (f) pH = 10, 1 layer.

Figure 4: The SEM of paper-Ag NPs were prepared in centrifuge tubes, hydroxylamine hydrochloride/sodium hydroxide solution pH = 7 or 10 and different layer of AgNPs.



(a,b) Relationship of Raman signal with pH (7--12). (c,d) pH = 7, Relationship of Raman signal with increasing number of nanoparticle (40, 80, 120, 160, 200 mL).

Figure 5: The SERS spectra of Preparation of paper--Ag NPs with 9: 1.

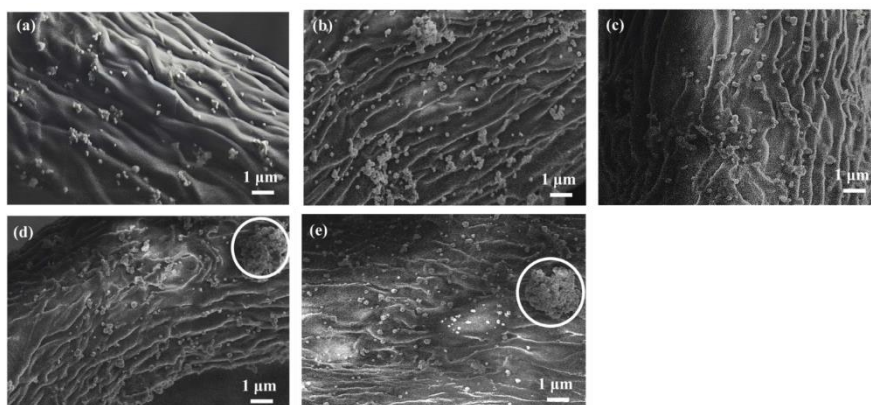


Figure 6: The SEM of paper--Ag NPs with different number of Ag NPs (40, 80, 120, 160, 200 mL) and pH = 7.

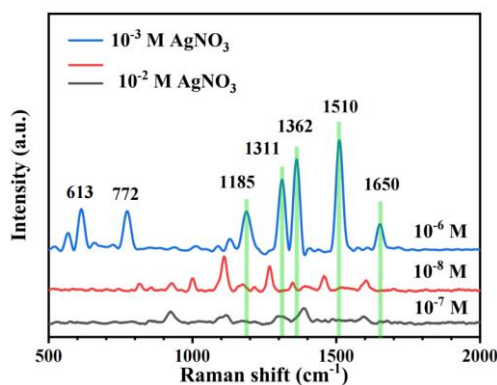
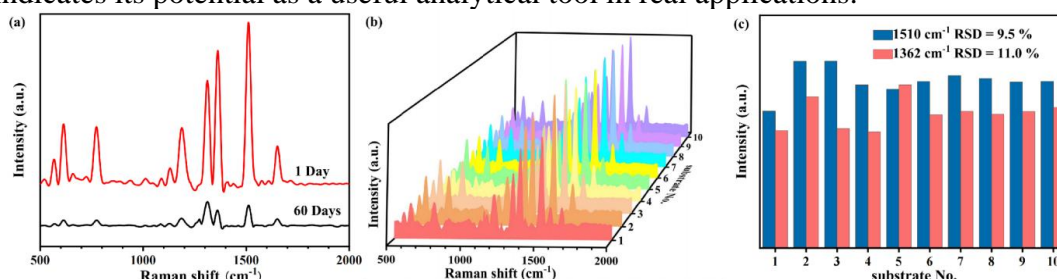


Figure 7: The SERS spectra of R6G (10⁻⁶, 10⁻⁸, 10⁻⁹ M) measured on substrates paper-Ag NPs prepared with different concentrations of AgNO₃ (1.11 × 10⁻³ M and 10⁻² M).

3.2. Stability and reproducibility

The SERS performance (stability and reproducibility) with the use of paper-Ag NPs was systematically investigated using the probe molecule R6G (10^{-6} M). The Figure 8a shows that the R6G (10^{-6} M) can still be detected after 60 days of storage in a refrigerator at 4 °C with good stability.

The SERS signals of 10 randomly selected paper Ag NPs were documented (Fig. 8b, c) to assess the reproducibility of the fabrication approach. The SERS intensities at 1510 cm^{-1} and 1362 cm^{-1} of the different paper Ag NPs showed an RSD value of 9.5 % and 11.0 %, respectively, indicating that the paper-based substrate is homogeneous. The excellent repeatability and reproducibility of this substrate indicates its potential as a useful analytical tool in real applications.



(a) Stability test of paper-Ag NPs substrates. (b) The SERS spectra of R6G collected from 10 different paper-Ag NPs substrate. (c) The corresponding SERS intensity variations of the peaks at 1362 and 1510 cm^{-1} on different substrates and RSD.

Figure 8: SERS spectra of R6G (10^{-6} M) measured on paper-Ag NPs substrate.

3.3. Application

The paper-Ag NPs can be cut as required and facilitating the detection of liquid samples. With the highest enhancement factor was used to explore its practical application (experimental conditions of pH = 7, 120 mL particle number). The Figure 9a is derived from Raman spectroscopy of a solid sample of ciprofloxacin on silicon wafers and the peaks are assigned as shown in Table 3[39,45,46]. The aromatic ring stretching mode at 1389 cm^{-1} is coupled to O–C–O, which can be used to characterise CIP. The Figure 9b shows the Raman spectrum of ciprofloxacin in 0.12 M HCl solution with a detection limit of 2.2×10^{-4} M. and demonstrated a simple linear increase with a logarithmic concentration of CIP from 4.75×10^{-2} to 4.75×10^{-4} M ($y = 1553.0840X - 8990.324$, $R^2 = 0.9998$) (Fig. 9c)

Table 3: Main Raman characteristic peaks and band assignments of CIP[39,45,46].

| SERS (cm^{-1}) | Band assignment |
|---------------------------|---|
| 635 – 695 | out-of-plane vibrations of the ring |
| 745 | represents the methylene rocking g |
| 1022 | C–H oscillation and pyrazine ring mixed vibrations |
| 1389 | symmetrical stretching vibration of the -COO- |
| 1458 | asymmetric stretching vibration of the benzene ring |
| 1534 | stretching vibration of the quinolone ring system |
| 1626 | asymmetric stretching vibration of aromatic ring C=O |

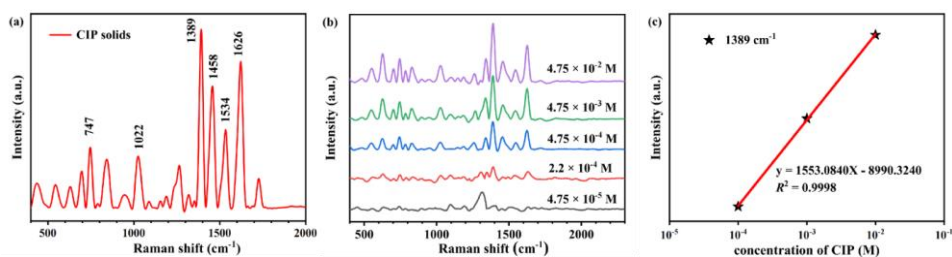


Figure 9: (a) SERS spectra of CIP solids measured Si. (b) Concentration-dependent SERS detection of CIP from 4.5×10^{-2} to 4.5×10^{-5} M. (c) The linear correlation of Raman intensity at 1389 cm^{-1} with the concentration changing from 10^{-2} to 10^{-4} M.

4. Conclusions

In summary, a simple, time-efficient and economical preparation method was developed for the preparation of plasma paper substrates with good flexibility, adsorption properties and SERS activity. The paper substrate was prepared using in situ growth of Ag NPs, and the Ag NPs were uniformly distributed inside and outside the paper, allowing random cutting and surface wiping extraction of the analyte, facilitating the detection of liquid samples. Most importantly, the substrate is a solution to the problem of paper swelling damage due to immersion. With an enhancement factor of 1.95×10^5 , detection of the R6G molecule 10^{-6} M can be achieved. A detection level of 2.2×10^{-4} M can be achieved for ciprofloxacin.

Acknowledgements

Thanks to my persistence.

References

- [1] Hu B, Pu H, Sun D-W. Multifunctional cellulose based substrates for SERS smart sensing: Principles, applications and emerging trends for food safety detection [J]. *Trends Food Sci Technol*, 2021, 110: 304-20.
- [2] Liu S, Guo J, Hinestroza J-P, et al. Fabrication of plasmonic absorbent cotton as a SERS substrate for adsorption and detection of harmful ingredients in food [J]. *Microchemical Journal*, 2021, 170: 106662.
- [3] Nilghaz A, Mahdi Mousavi S, Amiri A, et al. Surface-Enhanced Raman Spectroscopy Substrates for Food Safety and Quality Analysis [J]. *J Agric Food Chem*, 2022, 70(18): 5463-76.
- [4] Yan M, Li H, Li M, et al. Advances in Surface-Enhanced Raman Scattering-Based Aptasensors for Food Safety Detection [J]. *Journal of Agricultural and Food Chemistry*, 2021, 69(47): 14049-64.
- [5] Kang S, Wang W, Rahman A, et al. Highly porous gold supraparticles as surface-enhanced Raman spectroscopy (SERS) substrates for sensitive detection of environmental contaminants [J]. *RSC Advances*, 2022, 12(51): 32803-12.
- [6] Plou J, Molina-Martínez B, Garcá-Astrain C, et al. Nanocomposite Scaffolds for Monitoring of Drug Diffusion in Three-Dimensional Cell Environments by Surface-Enhanced Raman Spectroscopy [J]. *Nano Letters*, 2021, 21(20): 8785-93.
- [7] Mai Q D, Nguyen H A, Phung T L H, et al. Silver Nanoparticles-Based SERS Platform towards Detecting Chloramphenicol and Amoxicillin: An Experimental Insight into the Role of HOMO–LUMO Energy Levels of the Analyte in the SERS Signal and Charge Transfer Process [J]. *The Journal of Physical Chemistry C*, 2022, 126(17): 7778-90.
- [8] Wang H, Xue Z, Wu Y, et al. Rapid SERS Quantification of Trace Fentanyl Laced in Recreational Drugs with a Portable Raman Module [J]. *Analytical Chemistry*, 2021, 93(27): 9373-82.
- [9] Reokrungruang P, Chatnuntawech I, Dharakul T, et al. A simple paper-based surface enhanced Raman scattering (SERS) platform and magnetic separation for cancer screening [J]. *Sens Actuator B-Chem*, 2019, 285: 462-9.
- [10] Zhou Y, Li J, Zheng T, et al. Simple Plasma Test Based on a MoSe₂ SERS Platform for the Specific Diagnosis of Alzheimer's Disease [J]. *Chemical & Biomedical Imaging*, 2023, 1(2): 186-91.
- [11] Phung V-D, Kook J-K, Koh D Y, et al. Hierarchical Au nanoclusters electrodeposited on amine-terminated ITO glass as a SERS-active substrate for the reliable and sensitive detection of serotonin in a Tris-HCl buffer solution [J].

Dalton Transactions, 2019, 48(42): 16026-33.

[12] Yang Y, Long K, Kong F, et al. Surface-enhanced Raman spectroscopy on transparent fume-etched ITO-glass surface [J]. *Appl Surf Sci*, 2014, 309: 250-4.

[13] Abu Hatab N A, Oran J M, Sepaniak M J. Surface-Enhanced Raman Spectroscopy Substrates Created via Electron Beam Lithography and Nanotransfer Printing [J]. *ACS Nano*, 2008, 2(2): 377-85.

[14] Duan G, Lv F, Cai W, et al. General Synthesis of 2D Ordered Hollow Sphere Arrays Based on Nonshadow Deposition Dominated Colloidal Lithography [J]. *Langmuir*, 2010, 26(9): 6295-302.

[15] Chen P-J, Hsueh C-H. Imprintable Au-Based Thin-Film Metallic Glasses with Different Crystallinities for Surface-Enhanced Raman Scattering [J]. *The Journal of Physical Chemistry C*, 2021, 125(43): 23983-90.

[16] Jonker D, Srivastava K, Lafuente M, et al. Low-Variance Surface-Enhanced Raman Spectroscopy Using Confined Gold Nanoparticles over Silicon Nanocones [J]. *ACS Applied Nano Materials*, 2023, 6(11): 9657-69.

[17] Tran T T, Vu X H, Ngo T L, et al. Enhanced Raman scattering based on a ZnO/Ag nanostructured substrate: an in-depth study of the SERS mechanism [J]. *Physical Chemistry Chemical Physics*, 2023, 25(23): 15941-52.

[18] Juneja S, Singh J, Thapa R, et al. Improved SERS sensing on biosynthetically grown self-cleaning plasmonic ZnO nano-leaves [J]. *New Journal of Chemistry*, 2021, 45(44): 20895-903.

[19] Zhu W, Cai E-L, Li H-Z, et al. Precise Encoding of Triple-Bond Raman Scattering of Single Polymer Nanoparticles for Multiplexed Imaging Application [J]. 2021, 60(40): 21846-52.

[20] Toncheva A, Khelifa F, Paint Y, et al. Fast IR-Actuated Shape-Memory Polymers Using in Situ Silver Nanoparticle-Grafted Cellulose Nanocrystals [J]. *ACS Appl Mater Interfaces*, 2018, 10(35): 29933-42.

[21] Hesabi Z R, Allam N K, Dahmen K, et al. Self-Standing Crystalline TiO₂ Nanotubes/CNTs Heterojunction Membrane: Synthesis and Characterization [J]. *ACS Appl Mater Interfaces*, 2011, 3(4): 952-5.

[22] Huang Z, Meng G, Huang Q, et al. Large-area Ag nanorod array substrates for SERS: AAO template-assisted fabrication, functionalization, and application in detection PCBs [J]. 2013, 44(2): 240-6.

[23] Cheng L, Qian J, Ruan D, et al. Flexible and Highly Sensitive Sandwich-Structured PDMS with Silver Nanowires and Laser-Induced Graphene for Rapid Residue Detection [J]. *ACS Applied Polymer Materials*, 2023, 5(4): 2336-44.

[24] Zhu L, Dai H, Zhang S, et al. Enhanced Surface-Enhanced Raman Scattering (SERS) Sensitivity by the Self-Assembly of Silver Nanoparticles (Ag NPs) Laminated on Polydimethylsiloxane (PDMS) [J]. *Analytical Letters*, 2019, 52(18): 2868-82.

[25] Lee M, Oh K, Choi H-K, et al. Subnanomolar Sensitivity of Filter Paper-Based SERS Sensor for Pesticide Detection by Hydrophobicity Change of Paper Surface [J]. *ACS Sens*, 2018, 3(1): 151-9.

[26] Chang Y L, Su C J, Lu L C, et al. Aluminum Plasmonic Nanoclusters for Paper-Based Surface-Enhanced Raman Spectroscopy [J]. *Anal Chem*, 2022, 94(47): 16319-27.

[27] Wang S, Hao Q, Zhao Y, et al. Two-Dimensional Printed AgNPs@Paper Swab for SERS Screening of Pesticide Residues on Apples and Pears [J]. *J Agric Food Chem*, 2023, 71(12): 4982-9.

[28] Kim W, Kim Y H, Park H K, et al. Facile Fabrication of a Silver Nanoparticle Immersed, Surface-Enhanced Raman Scattering Imposed Paper Platform through Successive Ionic Layer Absorption and Reaction for On-Site Bioassays [J]. *ACS Appl Mater Interfaces*, 2015, 7(50): 27910-7.

[29] Sun M, Li B, Liu X, et al. Performance enhancement of paper-based SERS chips by shell-isolated nanoparticle-enhanced Raman spectroscopy [J]. *Journal of Materials Science & Technology*, 2019, 35(10): 2207-12.

[30] Das D, Senapati S, Nanda K K. "Rinse, Repeat": An Efficient and Reusable SERS and Catalytic Platform Fabricated by Controlled Deposition of Silver Nanoparticles on Cellulose Paper [J]. *ACS Sustain Chem Eng*, 2019, 7(16): 14089-101.

[31] Hou M, Li N, Tian X, et al. Preparation of SERS active filter paper for filtration and detection of pesticides residue from complex sample [J]. *Spectrochim Acta Pt B-Atom Spectr*, 2023, 285: 121860.

[32] Chen Y, Ge F, Guang S, et al. Low-cost and large-scale flexible SERS-cotton fabric as a wipe substrate for surface trace analysis [J]. *Appl Surf Sci*, 2018, 436: 111-6.

[33] Godoy N V, Garca-ujo D, Sigoli F A, et al. Ultrasensitive inkjet-printed based SERS sensor combining a high-performance gold nanosphere ink and hydrophobic paper [J]. *Sens Actuator B-Chem*, 2020, 320: 128412.

[34] Kumar A, Santhanam V. Paper swab based SERS detection of non-permitted colourants from dals and vegetables using a portable spectrometer [J]. *Anal Chim Acta*, 2019, 1090: 106-13.

[35] Jang W, Byun H, Kim J-H. Rapid preparation of paper-based plasmonic platforms for SERS applications [J]. *Mater Chem Phys*, 2020, 240: 122124.

[36] Yang Z, Chen G, Ma C, et al. Magnetic Fe₃O₄@COF@Ag SERS substrate combined with machine learning algorithms for detection of three quinolone antibiotics: Ciprofloxacin, norfloxacin and levofloxacin [J]. *Talanta*, 2023, 263: 124725.

[37] Yang L, Qin X, Jiang X, et al. SERS investigation of ciprofloxacin drug molecules on TiO₂ nanoparticles [J]. *Physical Chemistry Chemical Physics*, 2015, 17(27): 17809-15.

[38] Zhang A, Feng J, Yan J, et al. Laser reshaping of gold nanoparticles for highly sensitive SERS detection of

- ciprofloxacin [J]. *Appl Surf Sci*, 2022, 583: 152543.
- [39] Liu C, Müller-Böttcher L, Liu C, et al. Raman-based detection of ciprofloxacin and its degradation in pharmaceutical formulations [J]. *Talanta*, 2022, 250: 123719.
- [40] Kirchhoff J, Glaser U, Bohnert J A, et al. Simple Ciprofloxacin Resistance Test and Determination of Minimal Inhibitory Concentration within 2 h Using Raman Spectroscopy [J]. *Analytical Chemistry*, 2018, 90(3): 1811-8.
- [41] Nicolae L, Bernhard L. A New Method for Fast Preparation of Highly Surface-Enhanced Raman Scattering (SERS) Active Silver Colloids at Room Temperature by Reduction of Silver Nitrate with Hydroxylamine Hydrochloride. [J]. *J Am Chem Soc*, 2003, 107: 5723-7.
- [42] Cai J, Zhang L. Rapid dissolution of cellulose in LiOH/urea and NaOH/urea aqueous solutions [J]. *Macromol Biosci*, 2005, 5(6): 539-48.
- [43] Zhang Y, Liu R J, Ma X, et al. Ag nanoparticle decorated MnO₂ flakes as flexible SERS substrates for rhodamine 6G detection [J]. *RSC Advances*, 2018, 8(66): 37750-6.
- [44] Shao Y, Li S, Niu Y, et al. Three-Dimensional Dendritic Au–Ag Substrate for On-Site SERS Detection of Trace Molecules in Liquid Phase [J]. 2022, 12(12): 2002.
- [45] Son J, Kim G-H, Lee Y, et al. Toward Quantitative Surface-Enhanced Raman Scattering with Plasmonic Nanoparticles: Multiscale View on Heterogeneities in Particle Morphology, Surface Modification, Interface, and Analytical Protocols [J]. *Journal of the American Chemical Society*, 2022, 144(49): 22337-51.
- [46] Yang L, Qin X, Jiang X, et al. SERS investigation of ciprofloxacin drug molecules on TiO₂ nanoparticles [J]. *Phys Chem Chem Phys*, 2015, 17(27): 17809-15.